Recent advances with parallel FreeFEM

Pierre Jolivet — CNRS

December 9, 2021

FreeFEM days, 13th edition

1. Introduction
2. New functionalities
3. Applications
4. DD preconditioning
5. Conclusion

Introduction

Basic sequential functionalities

Domain specific language for FE

- mesh structure
- associated finite element spaces
- vector and matrix assemblies
- algebraic operations

Interface to other libraries

- installed by PETSc (`make petsc-slepc`)
  - MPICH
  - CMake
  - BLAS
  - MUMPS or SuperLU_DIST
  - SuperLU
  - SuiteSparse
  - *hypre*
  - METIS
  - ParMETIS
  - SCOTCH
  - TetGen
  - SLEPc
  - HPDDM
  - ARPACK
  - Mmg
  - ParMmg
  - Htool

Interface to other libraries

- installed by PETSc (`make petsc-slepc`)
  - MPICH
  - CMake
  - BLAS
  - MUMPS or SuperLU_DIST
  - SuperLU
  - SuiteSparse
  - *hypre*
  - METIS
  - ParMETIS
  - SCOTCH
  - TetGen
  - SLEPc
  - HPDDM
  - ARPACK
  - Mmg
  - ParMmg
  - Htool
- tested on Windows, Linux, Apple Intel/ARM, A64FX...

Interface to other libraries

- installed by PETSc (`make petsc-slepc`)
  - MPICH
  - CMake
  - BLAS
  - MUMPS or SuperLU_DIST
  - SuperLU
  - SuiteSparse
  - *hypre*
  - METIS
  - ParMETIS
  - SCOTCH
  - TetGen
  - SLEPc
  - HPDDM
  - ARPACK
  - Mmg
  - ParMmg
  - Htool
- tested on Windows, Linux, Apple Intel/ARM, A64FX...

$\Longrightarrow$ sequential or parallel (with FreeFem++-mpi)

Going parallel

- distributed-memory paradigm (MPI)
- not transparent to users
- additional lightweight macros

New functionalities

Important reminder

- examples, see `examples/hpddm/README.md`
- functionalities, see `CHANGELOG.md`
- developments are user-driven: ask what you need

Interpolation

- FreeFEM kernels are sequential
- interpolation between different fespaces

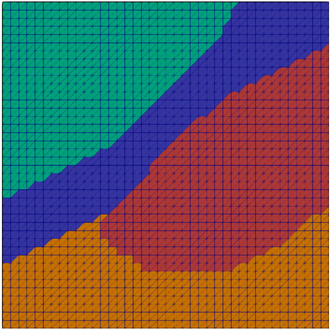

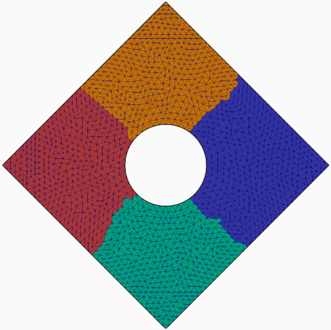

Interpolation

- FreeFEM kernels are sequential
- interpolation between different fespaces

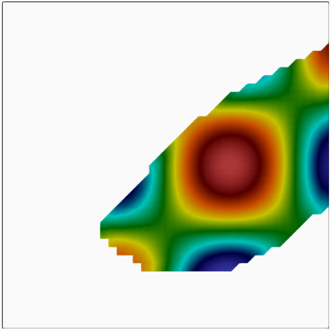

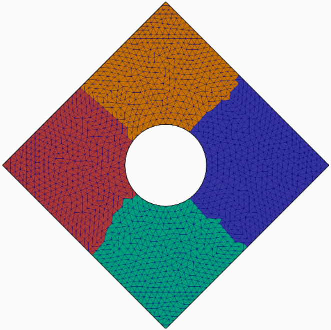

Interpolation

- FreeFEM kernels are sequential
- interpolation between different fespaces

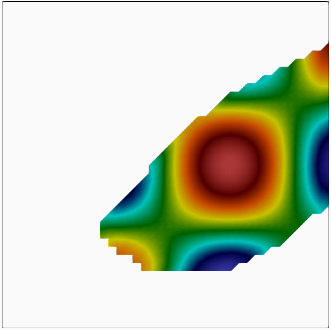

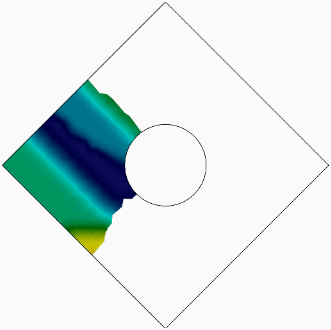

Parallel interpolation

- detect intersecting subdomains

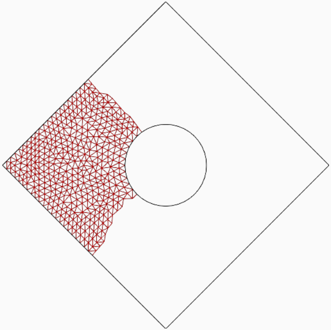

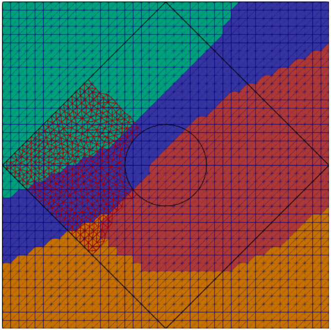

Parallel interpolation

- detect intersecting subdomains

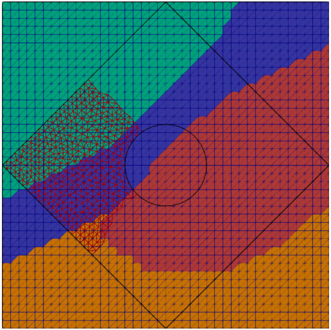

Parallel interpolation

- detect intersecting subdomains
- neighborwise reduction

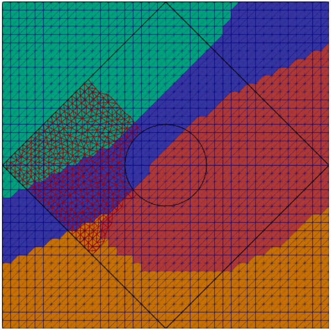

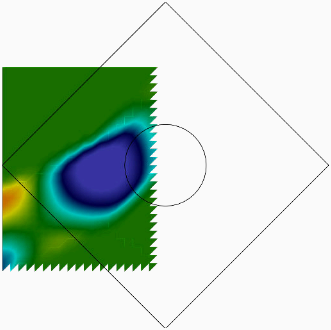

Parallel interpolation

- detect intersecting subdomains
- neighborwise reduction

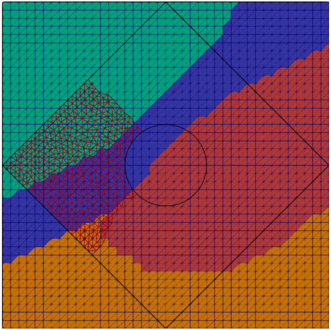

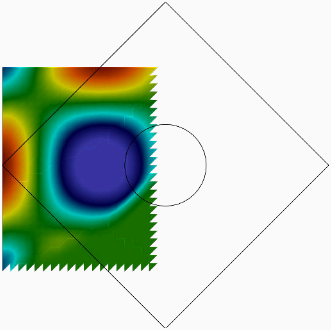

Parallel interpolation

- detect intersecting subdomains
- neighborwise reduction

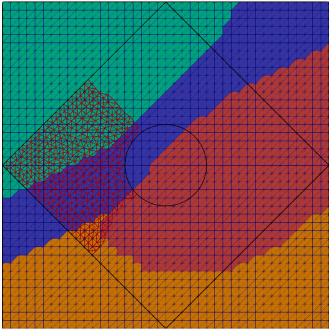

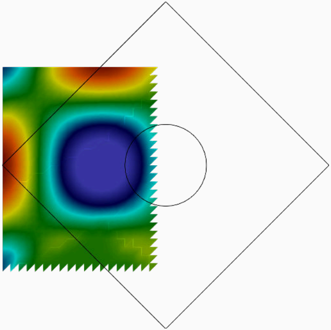

Parallel interpolation

- detect intersecting subdomains
- neighborwise reduction

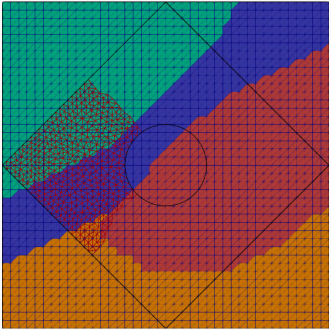

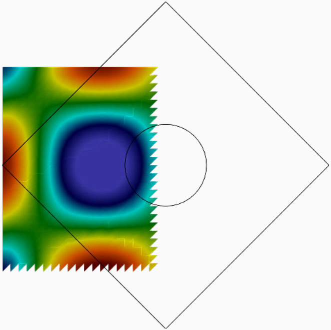

Parallel interpolation

- detect intersecting subdomains
- neighborwise reduction
- interpolation into the output fespace

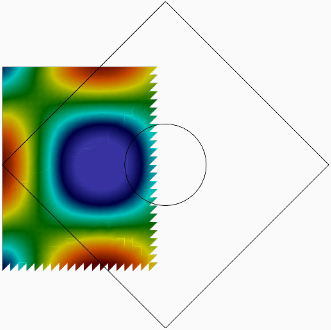

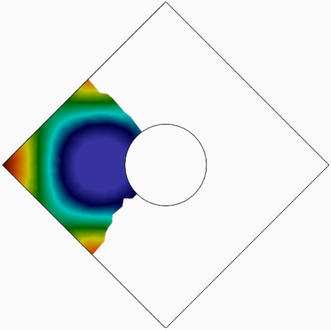

Parallel interpolation

- detect intersecting subdomains
- neighborwise reduction
- interpolation into the output fespace

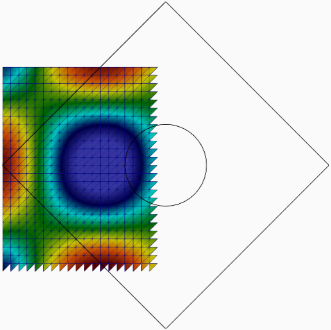

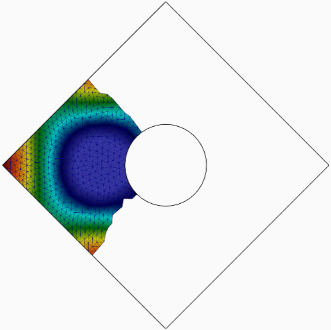

API for parallel interpolation

- transfer a single finite element function
- assemble a parallel `Mat`, like `interpolate`
- use with PETSc `PCMG` (GMG machinery)

API for parallel interpolation

- transfer a single finite element function
- assemble a parallel `Mat`, like `interpolate`
- use with PETSc `PCMG` (GMG machinery)

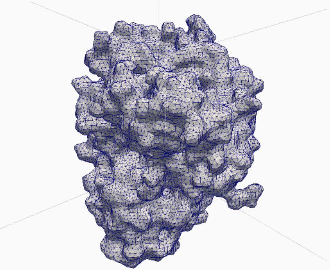

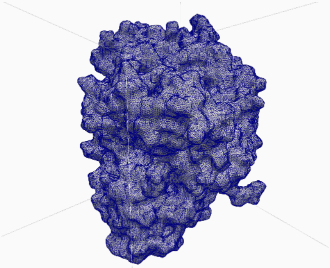

- 0.3M vs. 5M elements
- 61 `PCMG` iterations on 1,024 processes for Poisson
- 0.9 (nested) vs. 36 sec (non-nested) for building P

Parallel mesh adaptation

- Poisson equation on the Fischera corner
- algebraic system solved with *hypre*
- 78 MPI processes of Irène@TGCC

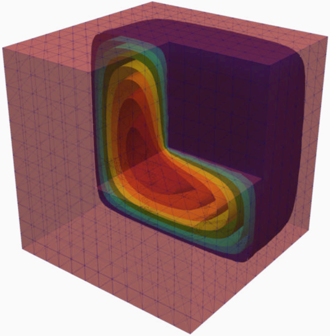

Parallel mesh adaptation

- Poisson equation on the Fischera corner
- algebraic system solved with *hypre*
- 78 MPI processes of Irène@TGCC

Iteration	#1
# of tetrahedra	45k
ParMmg (sec)	6.5
hypre (sec)	0.2

Parallel mesh adaptation

- Poisson equation on the Fischera corner
- algebraic system solved with *hypre*
- 78 MPI processes of Irène@TGCC

Iteration	#1	#2
# of tetrahedra	45k	47k
ParMmg (sec)	6.5	8.4
hypre (sec)	0.2	0.4

Parallel mesh adaptation

- Poisson equation on the Fischera corner
- algebraic system solved with *hypre*
- 78 MPI processes of Irène@TGCC

Iteration	#1	#2	#3
# of tetrahedra	45k	47k	93k
ParMmg (sec)	6.5	8.4	13.4
hypre (sec)	0.2	0.4	1.1

Parallel mesh adaptation

- Poisson equation on the Fischera corner
- algebraic system solved with *hypre*
- 78 MPI processes of Irène@TGCC

Iteration	#1	#2	#3	#4
# of tetrahedra	45k	47k	93k	249k
ParMmg (sec)	6.5	8.4	13.4	24.2
hypre (sec)	0.2	0.4	1.1	2.7

Parallel mesh adaptation

- Poisson equation on the Fischera corner
- algebraic system solved with *hypre*
- 78 MPI processes of Irène@TGCC

Iteration	#1	#2	#3	#4	#5
# of tetrahedra	45k	47k	93k	249k	715k
ParMmg (sec)	6.5	8.4	13.4	24.2	43.7
hypre (sec)	0.2	0.4	1.1	2.7	7.2

Parallel mesh adaptation

- Poisson equation on the Fischera corner
- algebraic system solved with *hypre*
- 78 MPI processes of Irène@TGCC

Iteration	#1	#2	#3	#4	#5	#6
# of tetrahedra	45k	47k	93k	249k	715k	2M
ParMmg (sec)	6.5	8.4	13.4	24.2	43.7	106
hypre (sec)	0.2	0.4	1.1	2.7	7.2	18

Parallel mesh adaptation

- Poisson equation on the Fischera corner
- algebraic system solved with *hypre*
- 78 MPI processes of Irène@TGCC

Iteration	#1	#2	#3	#4	#5	#6	#7
# of tetrahedra	45k	47k	93k	249k	715k	2M	5.5M
ParMmg (sec)	6.5	8.4	13.4	24.2	43.7	106	78.7
hypre (sec)	0.2	0.4	1.1	2.7	7.2	18	30

Parallel mesh adaptation

- Poisson equation on the Fischera corner
- algebraic system solved with *hypre*
- 78 MPI processes of Irène@TGCC

Iteration	#1	#2	#3	#4	#5	#6	#7	#8
# of tetrahedra	45k	47k	93k	249k	715k	2M	5.5M	12M
ParMmg (sec)	6.5	8.4	13.4	24.2	43.7	106	78.7	231
hypre (sec)	0.2	0.4	1.1	2.7	7.2	18	30	58

Parallel mesh adaptation

- Poisson equation on the Fischera corner
- algebraic system solved with *hypre*
- 78 MPI processes of Irène@TGCC

Iteration	#1	#2	#3	#4	#5	#6	#7	#8	#9
# of tetrahedra	45k	47k	93k	249k	715k	2M	5.5M	12M	26M
ParMmg (sec)	6.5	8.4	13.4	24.2	43.7	106	78.7	231	838
hypre (sec)	0.2	0.4	1.1	2.7	7.2	18	30	58	—

Nonstandard eigensolvers

- Nonlinear $T(\lambda)x = 0 \implies$ `NEPSolve`
- Polynomial $\left(\sum_{i=0}^{N} \lambda^i A_i\right)x = 0, N \geqslant 2 \implies$ `PEPSolve`
- SVD $Av = \sigma u \implies$ `SVDSolve`

Array of PETSc matrices

As easy as FreeFEM matrices, e.g., `Mat[int] A(N+1)`

Nonstandard eigensolvers

- Nonlinear $T(\lambda)x = 0 \implies$ `NEPSolve`
- Polynomial $\left(\sum_{i=0}^{N} \lambda^i A_i\right)x = 0, N \geqslant 2 \implies$ `PEPSolve`
- SVD $Av = \sigma u \implies$ `SVDSolve`

Array of PETSc matrices

As easy as FreeFEM matrices, e.g., `Mat[int] A(N+1)`

$\implies$ blasius-stability-1d-SLEPc-complex.edp

Easier use of shells for preconditioners

Oseen equations: $A = \begin{bmatrix} F & B \\ B^T & C \end{bmatrix} \Longrightarrow$

```
Mat A = [[F , B],
         [B', C]]
```

Easier use of shells for preconditioners

Oseen equations: $A = \begin{bmatrix} F & B \\ B^T & C \end{bmatrix} \implies$

```
Mat A = [[F , B],
         [B', C]]
```

```
Mat Object: 4 MPI processes
 type: nest
 rows=37507, cols=37507
  Matrix object:
   type=nest, rows=2, cols=2
   MatNest structure:
   (0,0) : prefix="fieldsplit_0_", type=mpiaij...
   (0,1) : type=mpiaij, rows=33282, cols=4225
   (1,0) : type=transpose, rows=4225, cols=33282
   (1,1) : prefix="fieldsplit_1_", type=mpiaij...
```

Easier use of shells for preconditioners

Oseen equations: $A = \begin{bmatrix} F & B \\ B^T & C \end{bmatrix} \Longrightarrow$

```
Mat A = [[F , B],
         [B', C]]
```

Triangular preconditioner: $\tilde{A} = \begin{bmatrix} \tilde{F} & B \\ 0 & \tilde{S} \end{bmatrix}$ with $\tilde{S}^{-1} \approx -M_p^{-1} F_p L_p^{-1}$

Easier use of shells for preconditioners

Oseen equations: $A = \begin{bmatrix} F & B \\ B^T & C \end{bmatrix} \implies$ `Mat A = [[F , B],`
`[B', C]]`

Triangular preconditioner: $\tilde{A} = \begin{bmatrix} \tilde{F} & B \\ 0 & \tilde{S} \end{bmatrix}$ with $\tilde{S}^{-1} \approx -M_p^{-1} F_p L_p^{-1}$

```
func real[int] PCD(real[int]& in) {
    real[int] out(in.n);
    KSPSolve(Lp,in,out); MatMult(Fp,out,in);
    KSPSolve(Mp,in,out); out *= -1.0;
    return out; // = -Mp \ Fp * Lp \ in
}
set(C, parent = A, precon = PCD,
       sparams = "-fieldsplit_1_pc_type shell");
```

FEM-BEM interoperability

- distributed FE space associated to a global numbering
- renumber the global mesh accordingly

FEM-BEM interoperability

- distributed FE space associated to a global numbering
- renumber the global mesh accordingly

```
Mat E,V;
ThLocal = ThGlobal;
createMat(ThLocal,E,P0); // elements
createMat(ThLocal,V,P1); // vertices
CoherentGlobalMesh(E,V,ThLocal,ThGlobal);
```

FEM-BEM INTEROPERABILITY

- distributed FE space associated to a global numbering
- renumber the global mesh accordingly

```
Mat E,V;
ThLocal = ThGlobal;
createMat(ThLocal,E,P0); // elements
createMat(ThLocal,V,P1); // vertices
CoherentGlobalMesh(E,V,ThLocal,ThGlobal);
```

FEM and/or BEM assemblies in a `Mat`

- `A = varfFEM()`, `int2d(ThLocal)`
- `A = varfBEM()`, `int2dx2d(ThGlobal)(ThGlobal)`

Example on a 2D geometry

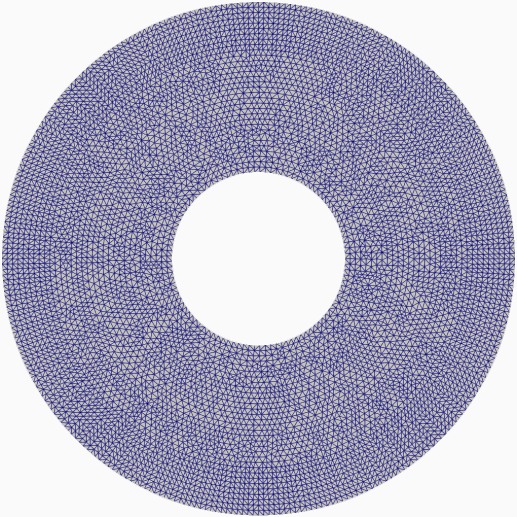

Unstructured circle with inclusion

Example on a 2D geometry

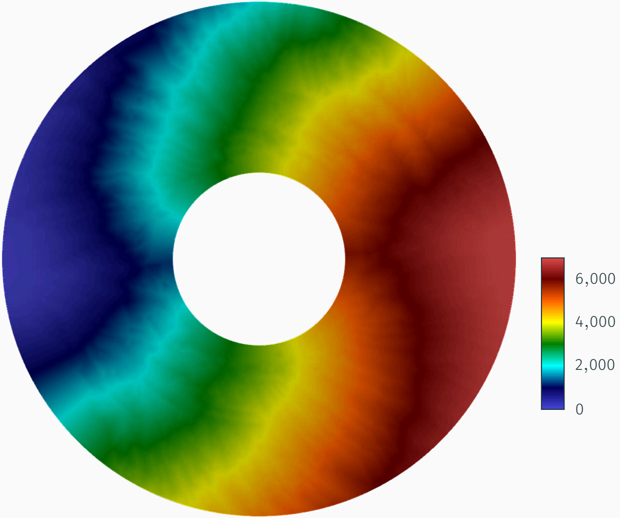

Canonical FreeFEM vertex numbering

Example on a 2D geometry

Domain decomposed mesh

Example on a 2D geometry

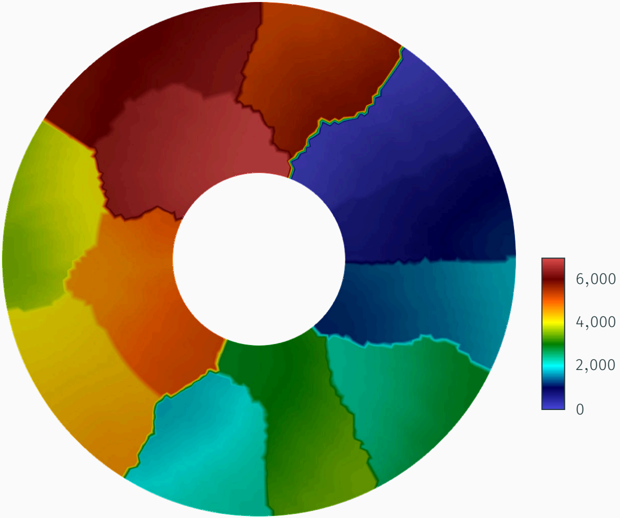

Coherent global FEM-BEM vertex numbering

Upcoming features/fixes

- `https://github.com/FreeFem/FreeFem-sources/pull/210`
- `https://community.freefem.org/t/dmplex-can-not-read-region-number/1368`
- ask and you shall receive

Applications

FEM-BEM COUPLING I

Solve the generalized eigenvalue problem for (u, λ):

$$\begin{bmatrix} A_k & D'_k - \frac{1}{2}M^{\mathrm{tr}} \\ M^{\mathrm{tr}} & -S_k \end{bmatrix} u = \lambda \begin{bmatrix} M & 0 \\ 0 & 0 \end{bmatrix} u$$

```
Mat<complex> C;
Sk *= -1.0;
C = [[Ak , R*TDkM]
     [F2B, Sk    ]];
```

FEM-BEM coupling I

Solve the generalized eigenvalue problem for (u, λ):

$$\begin{bmatrix} A_k & D'_k - \frac{1}{2}M^{\mathrm{tr}} \\ M^{\mathrm{tr}} & -S_k \end{bmatrix} u = \lambda \begin{bmatrix} M & 0 \\ 0 & 0 \end{bmatrix} u$$

```
Mat<complex> C;
Sk *= -1.0;
C = [[Ak , R*TDkM]
     [F2B, Sk    ]];
ObjectView(C);
```

```
Mat Object: 4 MPI processes
 type=nest, rows=2, cols=2
 MatNest structure:
 (0,0) : type=mpiaij, rows=10410, cols=10410
 (0,1) : type=composite, rows=10410, cols=...
 (1,0) : type=mpiaij, rows=1156, cols=10410
 (1,1) : type=htool, rows=1156, cols=1156
```

FEM-BEM coupling I

Solve the generalized eigenvalue problem for (u, λ):

$$\begin{bmatrix} A_k & D'_k - \frac{1}{2}M^{\text{tr}} \\ M^{\text{tr}} & -S_k \end{bmatrix} u = \lambda \begin{bmatrix} M & 0 \\ 0 & 0 \end{bmatrix} u$$

```
Mat<complex> C;
Sk *= -1.0;
C = [[Ak , R*TDkM]
     [F2B, Sk     ]];
ObjectView(C);
```

```
Mat Object: 4 MPI processes
  type=nest, rows=2, cols=2
  MatNest structure:
  (0,0) : type=mpiaij, rows=10410, cols=10410
  (0,1) : type=composite, rows=10410, cols=...
  (1,0) : type=mpiaij, rows=1156, cols=10410
  (1,1) : type=htool, rows=1156, cols=1156
```

$\Longrightarrow$ no need for shell to define block PC, use field-splitting

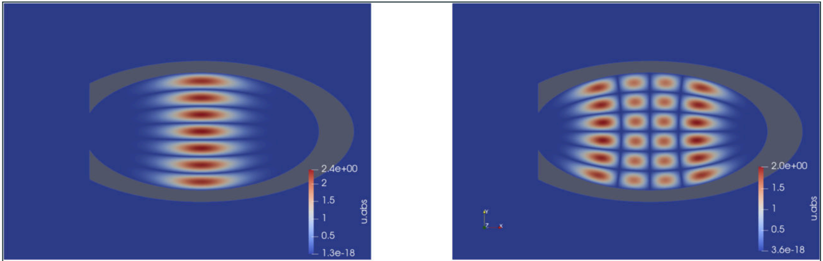

(c) $k^e_{3,0} = 22.526496854613104$ (d) $k^o_{2,4} = 22.6811692253925$

Figure 1.6: Absolute value of the eigenfunction of the truncated exterior Dirichlet problem associated with the smallest eigenvalue for the large cavity.

[Galkowski et al., 2021]

Mixed-precision for geophysics

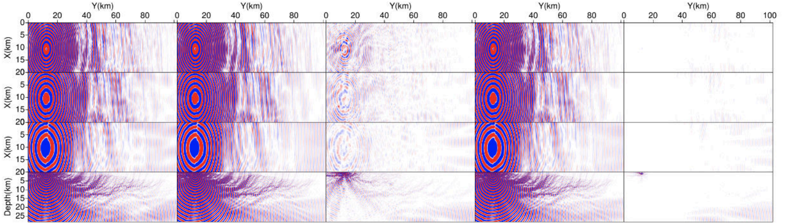

Figure 13: 3D GO_3D_OBS model. Comparison between the wavefields computed with the CBS, FEFD and FDFD methods. The rows show from top to bottom three depth slices at 6 km, 10 km and 16 km depth, and one vertical section at x=10 km. From left to right, the columns show the real part of the CBS wavefield, the FEFD wavefield, the differences between the two, the FDFD wavefield and its differences with the CBS wavefield.

[Tournier et al., 2021]

Semi-discretized RTE

$$\forall m \in [\![1; N_d]\!], \left(\vec{s}_m \cdot \nabla + (\kappa + \sigma)\right) I_m = \sigma \sum_{n=1}^{N_d} \omega_n \varphi_{m,n} \cdot I_n + \kappa B$$

Radiative transfer I

Semi-discretized RTE

$$\forall m \in [\![1; N_d]\!], \left(\vec{s}_m \cdot \nabla + (\kappa + \sigma)\right) I_m = \sigma \sum_{n=1}^{N_d} \omega_n \varphi_{m,n} \cdot I_n + \kappa B$$

$N_d = 80$

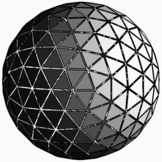

$N_d = 320$

$$\vec{s}_m = \begin{bmatrix} \sin\theta_m \cos\psi_m \\ \sin\theta_m \sin\psi_m \\ \cos\theta_m \end{bmatrix}$$

- κ (resp. σ) absorption (resp. scattering) coefficient
- φ phase scattering function
- B black body emissivity function

Radiative transfer II

[Kobayashi et al., 2001] benchmark

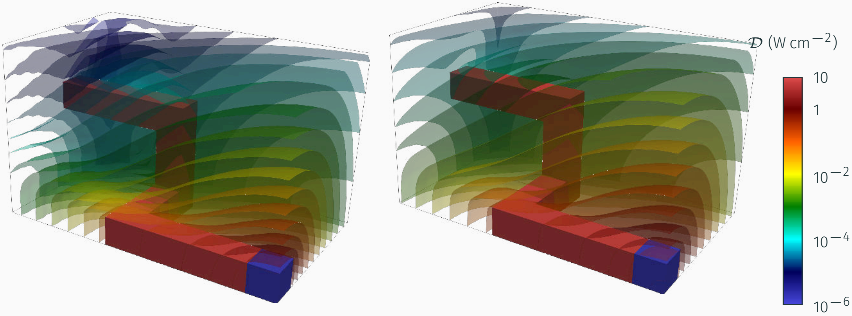

(a) Problem 3i

(b) Problem 3ii

Radiative transfer II

- GMVP [Nagaya et al., 2005]
- Ardra [Brown et al., 1999]

	Problem 3i			
y	Reference	MC	P_{21}	DOM
5	$5.96 \cdot 10^{0}$	$5.94 \cdot 10^{0}$	$5.96 \cdot 10^{0}$	$5.96 \cdot 10^{0}$
15	$1.37 \cdot 10^{0}$	$1.37 \cdot 10^{0}$	$1.34 \cdot 10^{0}$	$1.37 \cdot 10^{0}$
25	$5.01 \cdot 10^{-1}$	$5.01 \cdot 10^{-1}$	$4.95 \cdot 10^{-1}$	$5.00 \cdot 10^{-1}$
35	$2.52 \cdot 10^{-1}$	$2.53 \cdot 10^{-1}$	$2.49 \cdot 10^{-1}$	$2.50 \cdot 10^{-1}$
45	$1.50 \cdot 10^{-1}$	$1.50 \cdot 10^{-1}$	$1.56 \cdot 10^{-1}$	$1.48 \cdot 10^{-1}$
55	$9.92 \cdot 10^{-2}$	$9.92 \cdot 10^{-2}$	$1.20 \cdot 10^{-1}$	$9.84 \cdot 10^{-2}$
65	$4.23 \cdot 10^{-2}$	$4.23 \cdot 10^{-2}$	$5.10 \cdot 10^{-2}$	$4.20 \cdot 10^{-2}$
75	$1.15 \cdot 10^{-2}$	$1.15 \cdot 10^{-2}$	$8.91 \cdot 10^{-3}$	$1.14 \cdot 10^{-2}$
85	$3.25 \cdot 10^{-3}$	$3.25 \cdot 10^{-3}$	$1.95 \cdot 10^{-3}$	$3.33 \cdot 10^{-3}$
95	$9.48 \cdot 10^{-4}$	$9.49 \cdot 10^{-4}$	$6.82 \cdot 10^{-4}$	$9.69 \cdot 10^{-4}$

Radiative transfer II

- GMVP [Nagaya et al., 2005]
- Ardra [Brown et al., 1999]

	Problem 3ii		
y	MC	P_{21}	DOM
5	$8.62 \cdot 10^{0}$	$8.61 \cdot 10^{0}$	$8.63 \cdot 10^{0}$
15	$2.16 \cdot 10^{0}$	$2.13 \cdot 10^{0}$	$2.16 \cdot 10^{0}$
25	$8.94 \cdot 10^{-1}$	$8.84 \cdot 10^{-1}$	$8.93 \cdot 10^{-1}$
35	$4.78 \cdot 10^{-1}$	$4.72 \cdot 10^{-1}$	$4.74 \cdot 10^{-1}$
45	$2.89 \cdot 10^{-1}$	$2.99 \cdot 10^{-1}$	$2.87 \cdot 10^{-1}$
55	$1.93 \cdot 10^{-1}$	$2.24 \cdot 10^{-1}$	$1.91 \cdot 10^{-1}$
65	$1.05 \cdot 10^{-1}$	$1.19 \cdot 10^{-1}$	$1.04 \cdot 10^{-1}$
75	$3.38 \cdot 10^{-2}$	$3.02 \cdot 10^{-2}$	$3.35 \cdot 10^{-2}$
85	$1.08 \cdot 10^{-2}$	$8.54 \cdot 10^{-3}$	$1.08 \cdot 10^{-2}$
95	$3.40 \cdot 10^{-3}$	$2.83 \cdot 10^{-3}$	$3.40 \cdot 10^{-3}$

Radiative transfer — strong scaling

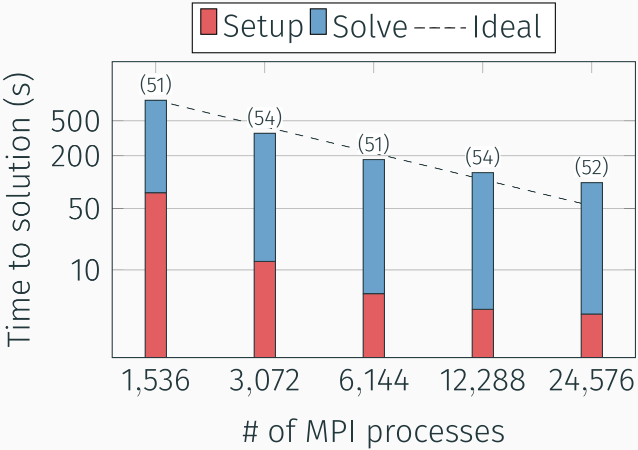

Nearly transparent medium, spherical inclusions, 13B unknowns (15M tets and $N_d = 5{,}120$), tolerance of 10^{-6}

Radiative transfer — weak scaling

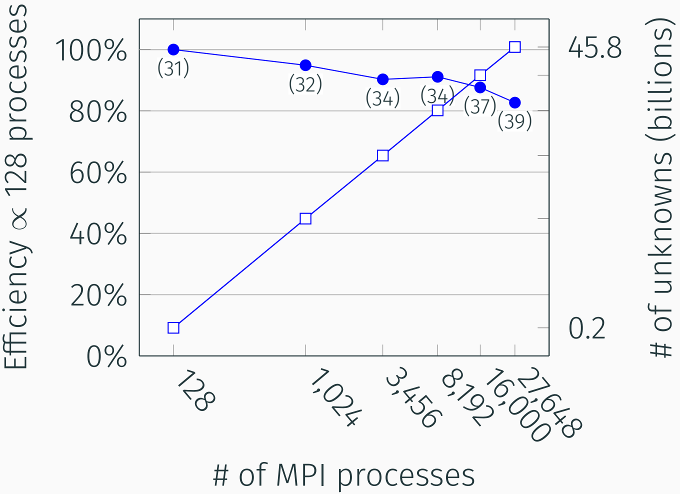

1.7M unknowns/processes ($N_d = 1{,}280$), 6 reflective surfaces, uniform spatial mesh refinement

Some more (tomorrow)

- A. Suzuki: “Shape optimization for a heat exchanger in Navier–Stokes flow [...]”
- M. Barzegari: “BioDeg: corrosion/biodegradation simulation software [...]”
- H. Li: “Topology optimization of a thermo-fluid system and an eigenfrequency problem [...]”

DD preconditioning

Robust domain decomposition method

- based on GenEO [Spillane et al., 2013]
- assembly of Neumann problems [Jolivet et al., 2021]
- nonlinear solve using SNES [Brune et al., 2015]

$$-\nabla \cdot (\kappa \nabla u) - 6.2e^u = 0$$

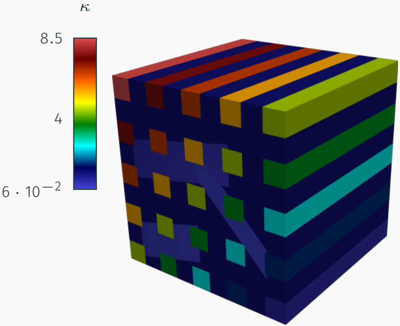

(a) Coefficient distribution

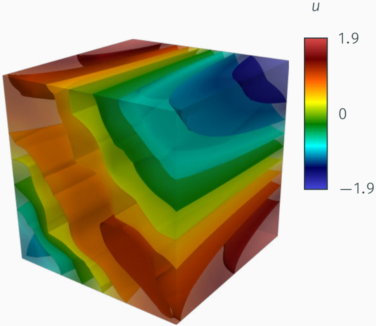

(b) Isosurfaces of the solution

Robust domain decomposition method

- based on GenEO [Spillane et al., 2013]
- assembly of Neumann problems [Jolivet et al., 2021]
- nonlinear solve using SNES [Brune et al., 2015]

$$-\nabla \cdot (\kappa \nabla u) - 6.2e^{u} = 0$$

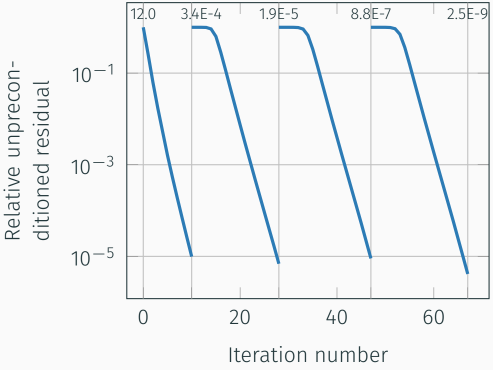

Algebraic preconditioning for least squares

Identifier	M^{-1}_{balanced}	M^{-1}_{ASM}	BoomerAMG	GAMG	`HSL_MI35`
mesh_deform	13	27	‡	35	**5**
EternityII_E	**43**	91	‡	63	199
lp_stocfor3	**34**	136	‡	513	211
deltaX	**23**	98	‡	784	640
sc205-2r	**54**	61	‡	195	97
stormg2-125	**42**	174	‡	†	†
Rucci1	**21**	484	118	364	†
image_interp	**11**	409	40	203	†
mk13-b5	19	21	**11**	‡	**11**
pds-100	18	202	**16**	35	110
fome21	20	104	**16**	20	41
sgpf5y6	224	264	‡	163	**110**
Hardesty2	**30**	913	88	404	†
Delor338K	**10**	11	‡	†	829
watson_2	**15**	109	‡	64	73
LargeRegFile	41	109	19	‡	**12**
cont11_l	**30**	490	53	723	‡

For nonsymmetric systems

$$\begin{aligned}\nabla \cdot (Vu) - \nu \nabla \cdot (\kappa \nabla u) &= 0 \text{ in } \Omega\\ u &= 0 \text{ in } \Gamma_0\\ u &= 1 \text{ in } \Gamma_1\end{aligned}$$

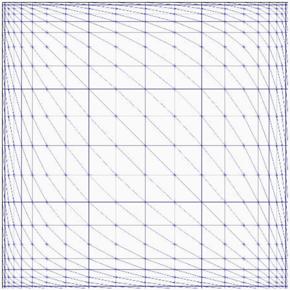

(a) Semi-structured mesh

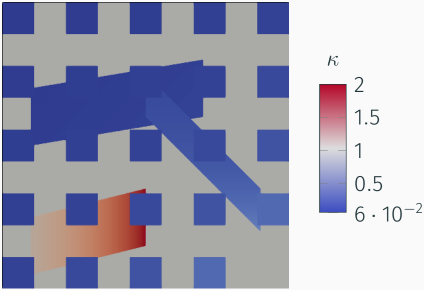

(b) Diffusivity coefficient κ

For nonsymmetric systems

$$
\begin{aligned}
\nabla \cdot (Vu) - \nu \nabla \cdot (\kappa \nabla u) &= 0 \text{ in } \Omega \\
u &= 0 \text{ in } \Gamma_0 \\
u &= 1 \text{ in } \Gamma_1
\end{aligned}
$$

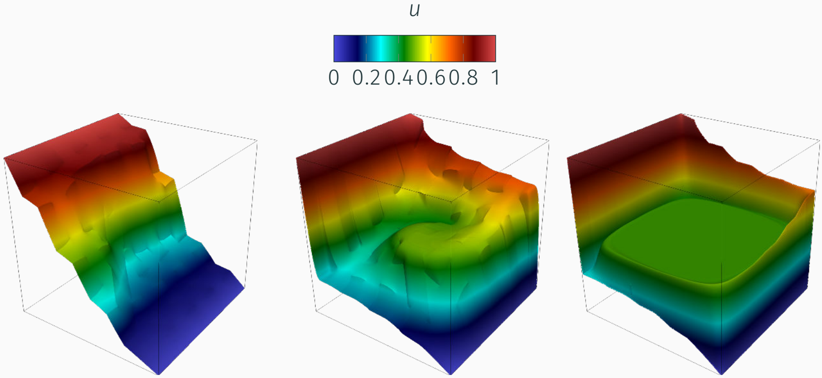

(a) $\nu = 1$ (b) $\nu = 10^{-2}$ (c) $\nu = 10^{-4}$

For nonsymmetric systems

$$\begin{aligned} \nabla \cdot (Vu) - \nu \nabla \cdot (\kappa \nabla u) &= 0 \text{ in } \Omega \\ u &= 0 \text{ in } \Gamma_0 \\ u &= 1 \text{ in } \Gamma_1 \end{aligned}$$

Dimension	k	N	n	ν 1	10^{-1}	10^{-2}	10^{-3}	10^{-4}
2	1	1,024	$6.3 \cdot 10^6$	23 (52,875)	20 (52,872)	19 (52,759)	20 (47,497)	21 (28,235)
3	2	4,096	$8.1 \cdot 10^6$	18 ($1.8 \cdot 10^5$)	14 ($1.8 \cdot 10^5$)	11 ($1.6 \cdot 10^5$)	16 (97,657)	29 (76,853)

For nonsymmetric systems

$$\nabla \cdot (Vu) - \nu \nabla \cdot (\kappa \nabla u) = 0 \text{ in } \Omega$$
$$u = 0 \text{ in } \Gamma_0$$
$$u = 1 \text{ in } \Gamma_1$$

Dimension	k	N	n	ν				
				1	10^{-1}	10^{-2}	10^{-3}	10^{-4}
2	1	1,024	$6.3 \cdot 10^6$	23 (52,875)	20 (52,872)	19 (52,759)	20 (47,497)	21 (28,235)
3	2	4,096	$8.1 \cdot 10^6$	18 ($1.8 \cdot 10^5$)	14 ($1.8 \cdot 10^5$)	11 ($1.6 \cdot 10^5$)	16 (97,657)	29 (76,853)

New algebraic preconditioning

- LS: [Al Daas, Jolivet, and Scott, 2021]
- SPD: [Al Daas and Jolivet, 2021]
- *M*-matrices: [Al Daas, Jolivet, and Rees, 2022]

Conclusion

Final words

- multiphysics solvers
  - high level of abstraction of FreeFEM
  - versatility of PETSc
- composability of solvers
- `http://joliv.et/FreeFem-tutorial`

Final words

- multiphysics solvers
  - high level of abstraction of FreeFEM
  - versatility of PETSc
- composability of solvers
- `http://joliv.et/FreeFem-tutorial`

Thank you!

References I

Al Daas, Hussam and Pierre Jolivet (2021). "A robust algebraic multilevel domain decomposition preconditioner for general sparse symmetric positive definite matrices". In: *SIAM Journal on Scientific Computing*, submitted for publication. URL: `https://arxiv.org/pdf/2109.05908.pdf`.

Al Daas, Hussam, Pierre Jolivet, and Jennifer A. Scott (2021). "A robust algebraic domain decomposition preconditioner for sparse normal equations". In: *SIAM Journal on Scientific Computing*, submitted for publication. URL: `https://github.com/prj-/aldaas2021robust`.

Brown, Peter N., Britton Chang, and Ulf R. Hanebutte (1999). *Spherical harmonic solutions to the 3D Kobayashi benchmark suite*. Tech. rep. Lawrence Livermore National Laboratory.

Brune, Peter R., Matthew G. Knepley, Barry F. Smith, and Xuemin Tu (2015). "Composing scalable nonlinear algebraic solvers". In: *SIAM Review* 57.4, pp. 535–565.

References II

Galkowski, Jeffrey, Pierre Marchand, and Euan A. Spence (2021). "Eigenvalues of the truncated Helmholtz solution operator under strong trapping". In: arXiv: `2101.02116 [math.AP]`.

Jolivet, Pierre, Jose E. Roman, and Stefano Zampini (2021). "KSPHPDDM and PCHPDDM: extending PETSc with robust overlapping Schwarz preconditioners and advanced Krylov methods". In: *Computers & Mathematics with Applications* 84, pp. 277–295. URL: `https://github.com/prj-/jolivet2020petsc`.

Kobayashi, Keisuke, Naoki Sugimura, and Yasunobu Nagaya (2001). "3D radiation transport benchmark problems and results for simple geometries with void region". In: *Progress in Nuclear Energy* 39.2, pp. 119–144.

Nagaya, Yasunobu, Keisuke Okumura, Takamasa Mori, and Masayuki Nakagawa (2005). *MVP/GMVP 2: general purpose Monte Carlo codes for neutron and photon transport calculations based on continuous energy and multigroup methods*. Tech. rep. Japan Atomic Energy Research Institute.

References III

Spillane, Nicole, Victorita Dolean, Patrice Hauret, Frédéric Nataf, Clemens Pechstein, and Robert Scheichl (2013). "Abstract robust coarse spaces for systems of PDEs via generalized eigenproblems in the overlaps". In: *Numerische Mathematik* 126.4, pp. 741–770.

Tournier, Pierre-Henri, Pierre Jolivet, Victorita Dolean, Hossein Aghamiry, Stéphane Operto, and Sebastián Riffo (2021). "Large-scale 3D frequency-domain wave simulation with finite-element and finite-difference methods and an optimized additive Schwarz domain-decomposition preconditioner: a tool for FWI of sparse node datasets". In: *Geophysics*, submitted for publication. URL: `https://arxiv.org/pdf/2110.15113.pdf`.